Ceramics International **24** (1998) 455–460

PII: S0272-8842(97)00035-7
0272-8842/98 $19.00+.00

Computer Simulation of Crack Propagation in Whisker-Reinforced Ceramic Composites

G. M. Song,* Y. Zhou, Y. Sun & T. C. Lei

School of Materials Science and Engineering, PO Box 433, Harbin Institute of Technology, Harbin 150001, People's Republic of China

(Received 23 July 1996; accepted 3 January 1997)

Abstract: A comprehensive computer program has been developed to simulate the process of crack propagation in whisker-reinforced ceramic composites. Two toughening mechanisms, crack bridging and crack deflection, are considered in the simulation. The fracture process of the composites is simulated in order to understand the complex mechanisms which occur between a propagating crack and whiskers. The results provided by the simulation indicate that there is a interaction between the two toughening mechanisms when they operate simultaneously. The values of the combined toughening are greater than that of each one individual toughening and less than their sum. With the increase of the whisker contents, the toughening effects of crack bridging and crack deflection increase, and the dominant toughening mechanism changes gradually from crack deflection to crack bridging. The best toughening effect can be obtained when whiskers are at high angles with the crack plane. The results of the simulation are in good agreement with that of the experiments for some ceramic composites. © 1998 Elsevier Science Limited and Techna S.r.l. All rights reserved

1 INTRODUCTION

Significant toughening has been achieved in many kinds of ceramics by the addition of whiskers.[1] Observations in the composites,[2–4] so far suggest that there are possibly five toughening mechanisms, crack bridging, crack deflection, whisker pullout, microcrack, and crack bowing. But there is still an ongoing debate about the relative importance of each of these mechanisms. A composite's fracture toughness depends not only on the characteristics of the separate components, and the way they are combined, but also on the role played by each of these factors during crack propagation. In most cases, more than one mechanism act simultaneously in a composite, but the relative contributions of each mechanism and roles for each material factor are very difficult to determine experimentally. It is a very valuable work to get this information using micromechanical models.

2 THEORETICAL MODELS

Microstructure observations of whisker-reinforced ceramic composites revealed that the major toughening mechanisms are crack bridging, whisker pullout and crack deflection. In this paper, the crack bridging model consists of two mechanisms, whisker bridging and whisker pullout.

When a crack meets with a whisker at a larger angle with the crack plane, the whisker will debond from the matrix and slip over a certain distance, L_s (Fig. 1). The relation between the axial stress, σ_ϕ, and the axial extension, μ_ϕ, of whisker into crack can be obtained according to the shear-lag model[5] by assuming that the incline whisker is not bending during the crack opening process.

*To whom correspondence should be addressed.

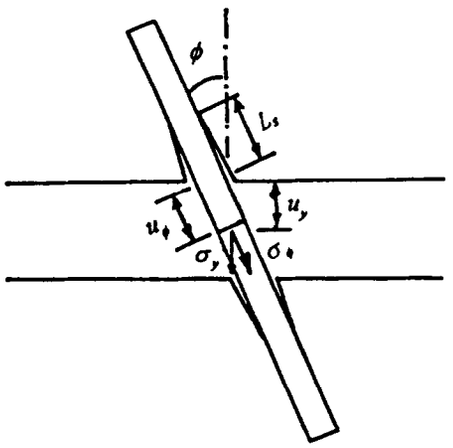

Fig. 1. Schematic of an incline whisker bridging and crack opening.

$$\sigma\phi = 2[e_w\tau(1+\eta)/r]^{1/2}\sqrt{u_\phi} \tag{1}$$

where $\eta = E_wV_w/(E_mV_m)$, E_w and r stand for the Young's modulus and the radius of the whisker, τ is the whisker–matrix interface shear stress.

By presuming that whisker failure will take place either within the crack surface or within the slipping zone, the strength along the whisker is given by

$$\begin{aligned} \sigma_{\phi,b} &= \sigma_w L/(2L_c) \quad (L \le L_c) \\ \sigma_{\phi,b} &= \sigma_w[1 - L_c/(2L)] \quad (L > L_c) \end{aligned} \tag{2}$$

where L_c is the whisker critical transfer length and L is the whisker length. Following the geometric relation

$$\sigma_y = \sigma_\phi \cos^2\phi, u_y = u_\phi \cos\phi \tag{3}$$

the relation between σ_y and u_y can be written as

$$\sigma_y = \lambda\sqrt{u_y} \tag{4}$$

where $\lambda = 2\cos^{3/2}\phi[E_w\tau(1+\eta)/r]^{1/2}$.

The crack closure stress perpendicular to the crack plane is obtained by

$$T_w = \sigma_y V_w \tag{5}$$

Crack deflection is commonly observed in whisker-reinforced ceramics. In the case of long whiskers where two ends of the whiskers are far from the crack plane, the crack is firstly deflected and propagates along with the whisker–matrix interface and returns to its original direction. The maximum deflected length of the crack is almost the same as maximum length of pulling out of the whisker, and much less than the half length of whisker.[3–6] The crack surface area is enlarged due to crack deflection, so the toughening effect associated with the crack surface area can be calculated. If the maximum deflection length, L_d, equals the slipping distance, L_s. The resultant toughness due to the additional surface area can be given by assuming that the fracture morphology comprises cones (height, 0 to L_d)

$$y_d/y_m = \frac{2}{\pi}\frac{2}{\delta}\int_0^{\pi/2}\sqrt{\left(\frac{\delta}{2}\right)^2 + (L_d\sin\theta)^2}\,d\theta \tag{6}$$

where Y_d, Y_m are the strain energy release rate of defected and undeflected crack, respectively, and δ is the centre to centre nearest neighbor spacing between whiskers.[7]

$$\delta \approx r\frac{e^{4Vw}}{V_w^{1/2}}\int_{4Vw}^{\infty} x^{1/2}e^{-x}dx \tag{7}$$

Figure 2 shows a cracked three-point bend specimen, the initial notch length, a_0, is much longer than the crack growing length, $(a - a_0)$, until the unstable propagation of the crack. We still assume that the whole crack behaviour as mode I crack, though the crack deflection takes place in the vicinity of the crack tip. As α is the angle between the crack faces, the crack open displacement at point x is given by

$$2u_y = \alpha(a - x) \qquad (a_o \le x \le a) \tag{8}$$

then the crack tip open displacement, *CTOD*, is obtained by

$$CTOD = \alpha(a - a_o) \tag{9}$$

When $u(x) \le u_{yc}$, the whisker will fail and the crack closure stress, $T_w(x) = 0$. The stress intensity factor, K_p, due to the external load, P, is

$$K_p = \frac{3PL}{2BW^2}\sqrt{a}F(a/W) \tag{10}$$

where $F(a/W)$ is a geometrical function.[8]

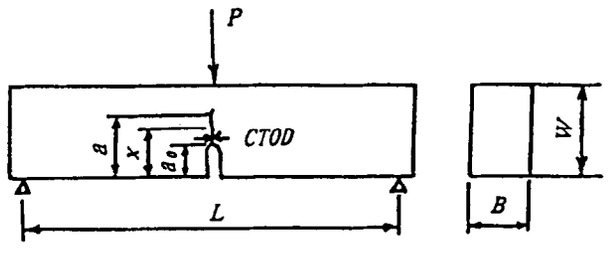

Fig. 2. Schematic of a single notch three-point bend specimen.

As a crack propagates, the fracture resistance, K_r, of the material is obtained by

$$K_r = K_m + dK_b + dK_d \tag{11}$$

where K_m is the fracture toughness of the matrix, dK_b is the shielding effect due to the crack closure stress, and dK_d is the additional toughness due to the additional crack surface area.

$$dK_d = \left(\sqrt{y_d/y_m} - 1\right) K_m \tag{12}$$

$$dK_b = \int_{a_0}^{a} \frac{2T_w(u_y(x))}{\sqrt{\pi a}} H(a/W, x/a) \tag{13}$$

where $H(a/W, x/a)$ is a geometrical function.[8]

3 SIMULATION RESULTS AND DISCUSSION

These parameters of $ZrO_2(6mol\%Y_2O_3)/SiC_w$ ceramic composites are used to simulate the fracture process of a three-point bend specimen. $r = 0.5\,\mu m$, $E_m = 230\,GPa$, $E_w = 550\,GPa$, $\sigma_w = 8\,GPa$,[9] $L_w = 25\mu m$, $K_m = 3.42\,MPa\,m^{1/2}$, the interface shear stress, τ, is given by[10]

$$\tau = -\mu\Delta\alpha\Delta T[(1 + \nu_m)/2E_m + (1 - 2\nu_w)/E_w] \tag{14}$$

where $\Delta\alpha$ denoted the coefficient of thermal expansion, ν is Poisson's ratio, ΔT is the temperature differential between the temperature below which stress relaxation cannot take place and the temperature under consideration. μ is the friction coefficient of the interface and is taken as 0.5 when the whisker surface is not treated.

It is assumed that the whisker angles, φ, are uniformly distributed from 0 to Φ (see Fig. 1) and Φ is $\pi/2$. The initial crack, a_0, is 2 mm and the width, W, of the sample is 4 mm. The load, P, associated with an applied stress intensity, K_p, is given by eqn (10), the crack resistance, K_r, can also be given by eqn (11). If $K_p < K_r$, the applied stress intensity, K_p, is increased. If $K_p = K_r$, the main crack, a, is allowed to extend by a small increment, $da(= a_0/1000)$, all the stress calculations are repeated and the process is redone until the main crack propagates in a unstable manner.

Figure 3(a) and (b) gives a representative view of the way in which a crack propagates through a matrix containing randomly dispersed whiskers.

When a crack propagates through a matrix containing whiskers, the crack bridging zone is formed behind the crack tip and the crack deflects, which decreases greatly the stress intensity at the crack tip, the further propagation of the crack then requires an higher load, P. As P increases, *CTOD* increases and some bridging whiskers will fail, which leads K_r to drop. Once the crack stress intensity factor, K_p is higher than K_r, the crack will propagate and the applied load, P will drop, but crack propagation is immediately arrested as the load increase is resumed. Figure 4 shows the calculated fracture resistance curves of ZrO_2/SiC_w composites, and Fig. 5 shows the corresponding load–crack length curves. It is found that the extension of a crack proceed in an irregular manner by repeated initiation and arrest, and the load-displacement curve exhibits a sawtooth shape (see Fig. 6).

Figure 7 shows that relative toughness of crack bridging and crack deflection are all increased with the increase of the whisker contents, but there is a significant difference between both increasing extensions of crack bridging and crack deflection, as shown in Fig. 8. The results of the simulation indicate that dominant toughening mechanism is changed gradually from crack deflection to crack bridging with increasing the whisker contents. There is an interaction between crack bridging and

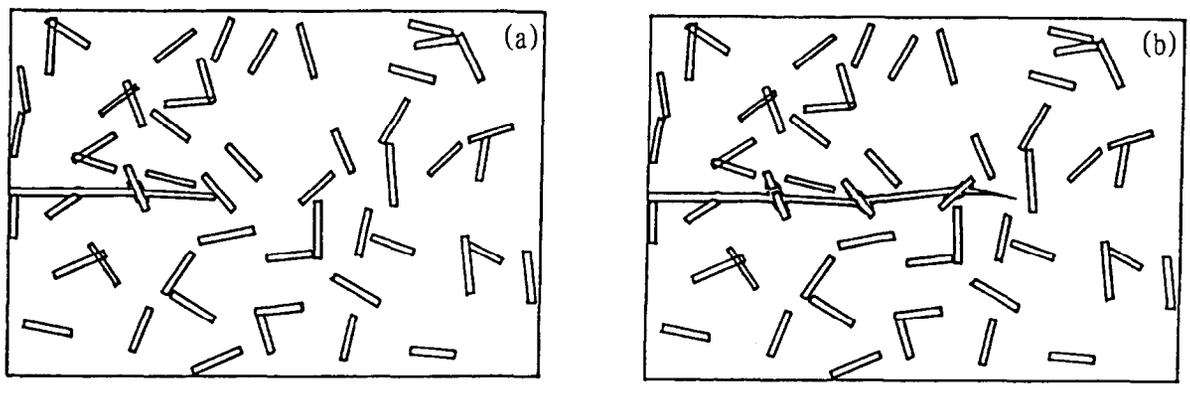

Fig. 3. A representative simulation view of a crack propagation in whisker-reinforced ceramic composites.

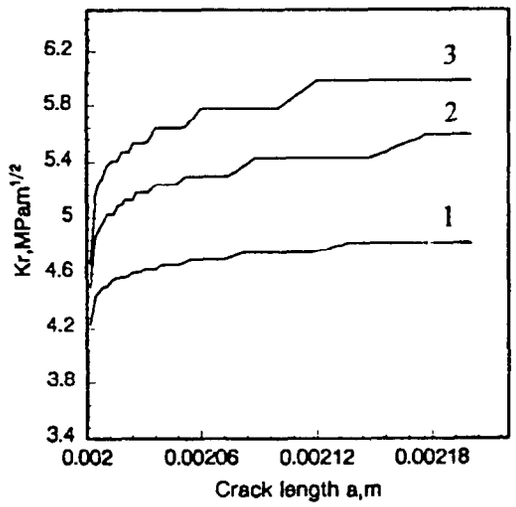

Fig. 4. R curves showing the dependence of the whisker contents: (1) 10% SiC_w; (2) 20% SiC_w; (3) 30% SiC_w.

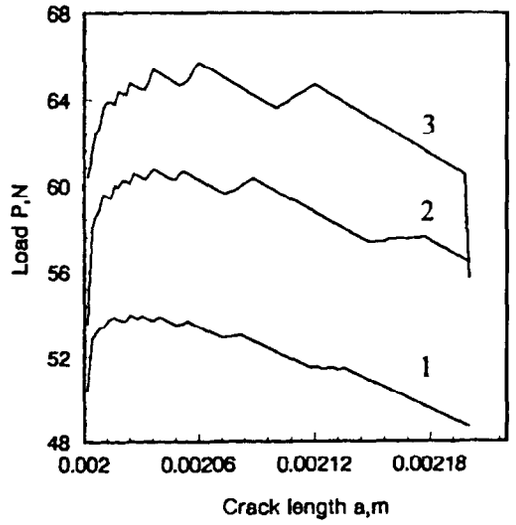

Fig. 5. Load (P)-crack length curves showing the sawtooth shape arising from the crack bridging process: (1) 10% SiC_w; (2) 20% SiC_w; (3) 30% SiC_w.

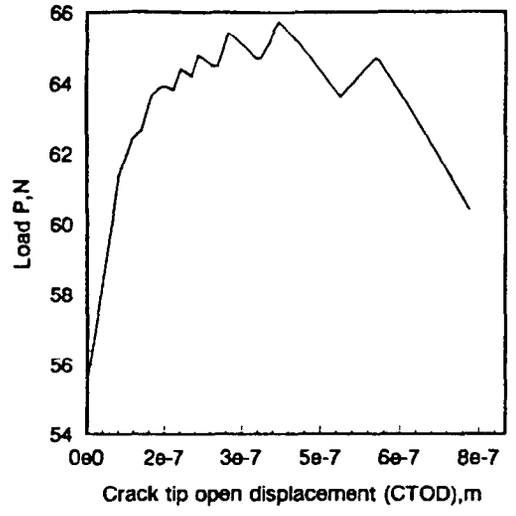

Fig. 6. A load (P)-displacement CTOD curve showing the sawtooth shape arising from the crack bridging process (ZrO_2/30% SiC_w).

crack deflection when they operate simultaneously, the combined toughening effects are greater than the individual toughening effects when either toughening method acts alone, but less than their sum, as shown in Fig. 7 and Table 1, that may be due to the negative interaction between the two toughening mechanisms.

When the angle, Φ (see Fig. 1) is taken as different value from 0 to $\pi/2$, the influence of whisker orientation on the toughening of crack bridging can be computed, as shown in Fig. 9, so the preferred orientation of whisker can be utilised for higher toughening.

4 COMPARISON WITH EXPERIMENTAL RESULTS

The ZrO_2(6mol%Y_2O_3)/SiC_w ceramic composites(with 10, 20 and 30 vol% SiC_w) are manufactured by hot-pressing method. The fracture toughness was measured with an Instron-1186 testing machine using the single notch three-point bend specimens 20×4×2 mm which have $a_0 = 2$ mm, $B = 2$ mm, $W = 4$ mm and $L = 16$ mm, and crack propagation path and fracture morphologies were observed on an S-570 type SEM.

SEM micrograph shows that major toughening mechanisms are crack bridging and crack deflection, both mechanisms are shown in Fig. 10(a) and (b).

The experimental results and the simulation results are given in Table 1, these data indicate the predicted fracture toughness values, K^*_{IC}, of combined toughening are in good agreement with the experimental values, K_{IC}.

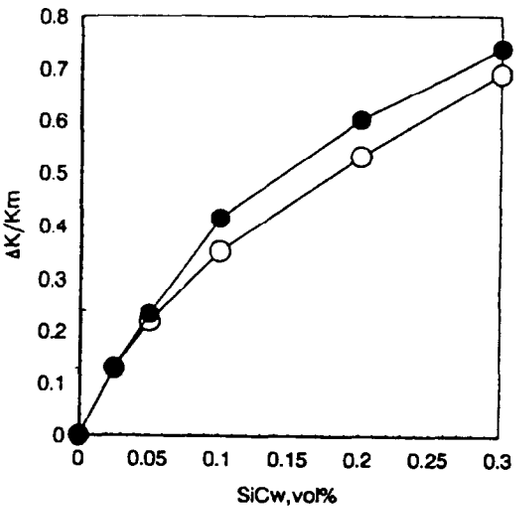

Fig. 7. Effect of the whisker contents on the relative toughness of combined toughening. ○, the combined toughening effect; ●, the sum of the individual toughening.

Table 1. Fracture toughening predictions (MPa m$^{1/2}$)

SiC_w	Predicted				Measured
(vol%)	Toughening by crack deflection ΔK_d	Toughening by crack bridging ΔK_b	Sum K'_{IC} $K_m+\Delta K_b+\Delta K_d$	Predicted K^*_{IC} (by combined toughening)	K_{IC}
0					3.42($=K_m$)
10	0.794	0.63	1.424+3.42=4.844	1.21+3.42=4.63	4.43±0.15
20	1.048	1.01	2.058+3.42=5.500	1.82+3.42=5.24	4.89±0.36
30	1.191	1.39	2.581+3.42=6.001	2.36+3.42=5.78	5.79±0.15

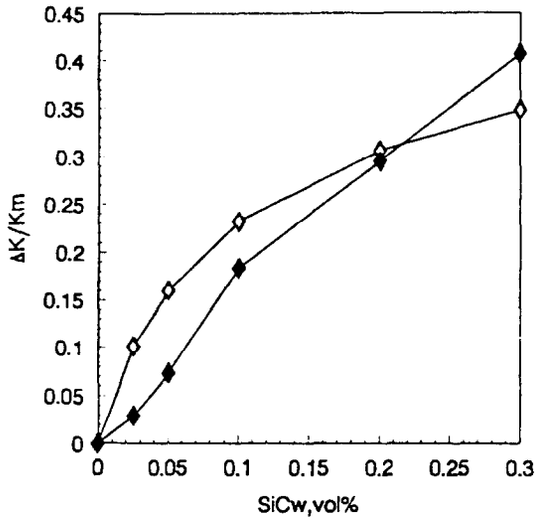

Fig. 8. Effect of whisker content on the relative toughness of crack bridging and crack deflection. ◇, Crack deflection; ◆, crack bridging.

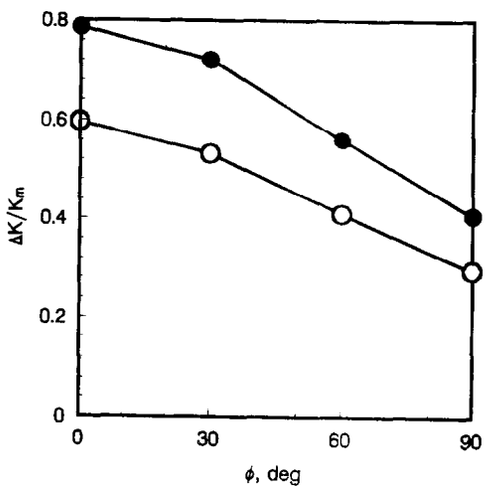

Fig. 9. Effect of orientation distribution of whiskers on the crack bridging toughening effect. ○, with 20% SiC_w; ●, with 30% SiC_w.

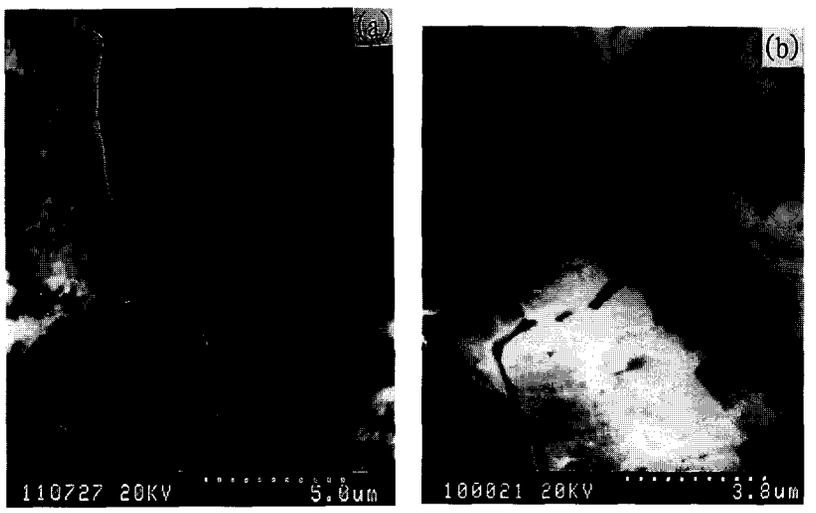

Fig. 10. SEM micrographs of composites (a) with 20% SiC_w showing the bridging of the whisker and (b) with 20% SiC_w showing crack deflection.

5 SUMMARY AND CONCLUSIONS

Developed in this work is a model that simulates the crack propagating in whisker-reinforced ceramic composites where the interaction between the crack and whiskers is included. The model is valid by comparing the predicted toughening values with the experimental toughening values. The results provided by the simulation indicate:

1. There is a interaction between crack bridging and crack deflection when they operate simultaneously. The combined toughening effects are greater than the individual toughening

effects when either toughening method acts alone, but less than their sum.
2. Increasing the whisker contents, the toughening effects of both crack bridging and crack deflection increase and the dominant toughening mechanism is changed gradually from crack deflection to crack bridging.
3. The fracture toughness is increased when the orientation of whisker extends to be perpendicular to the crack plane.

REFERENCES

1. BECHER, P. F. & WEI, G. C., Toughening behavior in SiC whisker-reinforced alumina. *J. Am. Ceram. Soc.*, **67** (1984) C267.
2. FABER, K. T. & EVANS, A. G., Crack deflection process–I. Theory. *Acta Metall.*, **31** (1983) 565–576.
3. LIN, G. Y., LEI, T. C., ZHOU, Y. & WANG, S. X., Microstructure and mechanical properties of SiC whisker reinforced ZrO_2(6mol%Y_2O_3) composites. *Mater. Sci. Tech.*, **9** (1993) 651–664.
4. BENGISU, M., INAL, O. T. & TOSYALI, O., On whisker toughening in ceramic materials. *Acta Metall. Mater.*, **39** (1991) 2509–2517.
5. MARSHALL, D. B., COX, B. N. & EVANS, A. G., The mechanics of matrix cracking in brittle-matrix fiber composites. *Acta Metall.*, **33** (1985) 2013–2021.
6. ZHOU, Y., ZHU, W. Z. & LEI, T. C., Mechanical properties and toughening mechanisms of SiC_w/ZrO_2 ceramic composites. *Ceram. Int.*, **18** (1992) 141–145.
7. BANSAL, P. P. & ARDELL, A. J., Average nearest-neighbor distances between uniformly distributed finite particles. *Metallography*, **5** (1972) 97–111.
8. TADA, H., PARIS, P. C. & IRWIN, G. R., *The Stress Analysis of Cracks Handbook*. Del Research Corporation, Hellertown, PA., 1973, pp.2, 16–27.
9. EKINAGA, N., Characteristics of SiC whisker and their applications. *Proc. 1st Japan International SAME Symposium*, 1989, pp. 883–888.
10. BECHER, P. F., TIEGS, T. N., OGLE J. C. & WARWICK, W. H., Toughening of ceramics by whisker reinforcement. In *Fracture Mechanics of Ceramics*, vol. 7, ed. R. C. Bradt, A. G. Evans, D. P. Hasselman and F. F. Lange. Plenum Press, New York, 1986, pp. 639–649.